Structure
Article

Two-State Conformations in the Hyaluronan-Binding Domain Regulate CD44 Adhesiveness under Flow Condition

Shinji Ogino,[1] Noritaka Nishida,[1] Ryo Umemoto,[1] Miho Suzuki,[1] Mitsuhiro Takeda,[1] Hiroaki Terasawa,[1] Joji Kitayama,[2] Masanori Matsumoto,[3] Haruko Hayasaka,[3] Masayuki Miyasaka,[3] and Ichio Shimada[1,4,*]
[1]Graduate School of Pharmaceutical Sciences
[2]Graduate School of Medicine
The University of Tokyo, Hongo, Bunkyo-ku, Tokyo 113-0033, Japan
[3]Laboratory of Immunodynamics, Department of Microbiology and Immunology, Osaka University Graduate School of Medicine, 2-2 Yamada-oka, Suita 565-0871, Japan
[4]Biomedicinal Information Research Center, National Institute of Advanced Industrial Science and Technology, Aomi, Koto-ku, Tokyo 135-0064, Japan
*Correspondence: shimada@iw-nmr.f.u-tokyo.ac.jp
DOI 10.1016/j.str.2010.02.010

SUMMARY

The hyaluronan (HA) receptor CD44 mediates cell adhesion in leukocyte trafficking and tumor metastasis. Our previous nuclear magnetic resonance (NMR) studies revealed that the CD44 hyaluronan-binding domain (HABD) alters its conformation upon HA binding, from the ordered (O) to the partially disordered (PD) conformation. Here, we demonstrate that the HABD undergoes an equilibrium between the O and PD conformations, in either the presence or absence of HA, which explains the seemingly contradictory X-ray and NMR structures of the HA-bound HABD. An HABD mutant that exclusively adopts the PD conformation displayed a higher HA affinity than the wild-type. Rolling of the cells expressing the mutant CD44 was less efficient than those expressing the wild-type, due to the decreased tether frequency and the slow cellular off rate. Considering that the mutant CD44, devoid of the low-affinity state, exhibited impaired rolling, we conclude that the coexistence of the high- and low-affinity states of the HABD is essential for the CD44-mediated rolling.

INTRODUCTION

CD44 is a principal cell surface receptor for hyaluronan (HA), a major glycosaminoglycan component of the extracellular matrix (Aruffo et al., 1990). Cell adhesion and migration mediated by CD44 are implicated in a wide variety of biological and pathological events, including hematopoiesis, lymphocyte activation and homing, and tumor-cell migration and metastasis (Naor et al., 1997; Sugahara et al., 2006, 2003). CD44 expressed on lymphocytes mediates rolling adhesion on endothelial cells displaying HA under flow conditions (Clark et al., 1996; DeGrendele et al., 1996). Rolling adhesion is an important first step for the recruitment of leukocytes from the bloodstream to inflammatory sites and the secondary lymphoid organs and is only mediated by specialized adhesion molecules, such as selectins or α4 integrins (Alon et al., 1995b; Chen et al., 1997).

CD44 is a type I transmembrane glycoprotein receptor. The extracellular portion of CD44 comprises an N-terminal hyaluronan-binding domain (HABD), followed by a heavily glycosylated and alternatively spliced stem region. The short cytoplasmic tail of CD44 is connected to the actin cytoskeleton via ERM (ezrin, radixin, and moesin) proteins (Tsukita et al., 1994). The CD44 HABD contains a Link module, which is conserved among many other HA-binding proteins, including tumor necrosis factor stimulating gene-6 (TSG6) (Day and Prestwich, 2002). In addition, the N- and C-terminal flanking regions are necessary for the proper folding and the HA-binding activity of the HABD (Banerji et al., 1998; Peach et al., 1993). The three-dimensional structures of the HABD in the ligand-free state, revealed by the X-ray and nuclear magnetic resonance (NMR) studies, demonstrated that the Link module and the N- and C-terminal extensions form a single folded unit, which is composed of three α helices and eleven β strands, arranged in the order of β0-β0'-β1-α1-α2-β3-β4-β5-β6-β7-β8-β9-α3 (Takeda et al., 2003; Teriete et al., 2004).

We recently determined the solution structure of the HABD of human CD44 in complex with an HA hexamer (HA6) and demonstrated that HA binding induces an allosteric conformational rearrangement of the HABD, in which the C-terminal β9 strand and α3 helix become unstructured and the β8 strand is rearranged with respect to the β0 strand (Takeda et al., 2006). In addition, the heteronuclear NOE experiments showed that the C-terminal segment of the HABD has enhanced flexibility in the HA-bound state. Therefore, we refer to the conformation of the HABD in the unbound and HA-bound states as the ''ordered (O)'' and the ''partially disordered (PD)'' conformations, respectively, on the basis of the conformational differences in the C-terminal segment. However, the subsequently solved crystal structures of the HABD of mouse CD44 in complex with HA8 adopted the O conformation (Banerji et al., 2007). Therefore,

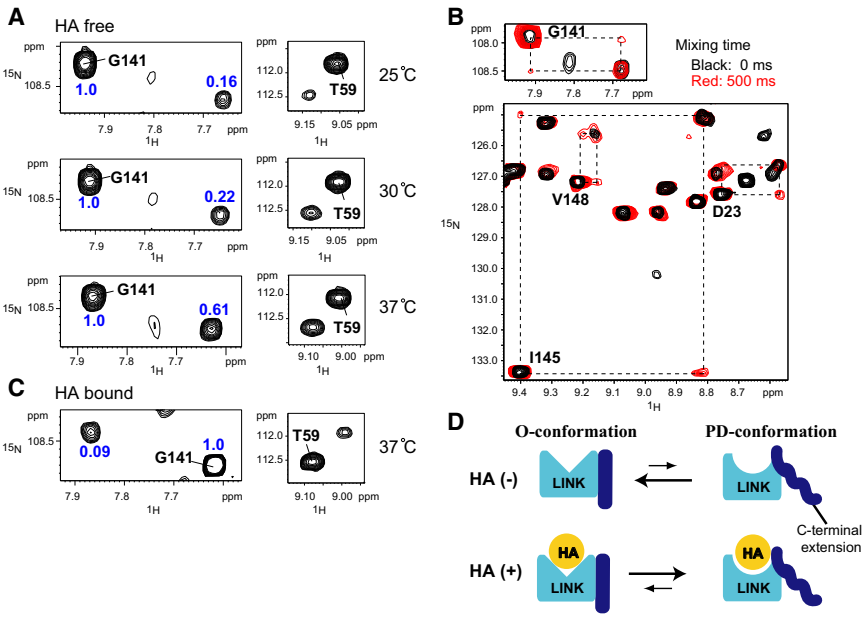

Figure 1. Two-State Conformational Equilibrium of CD44 HABD

(A) Selected regions of the ^{1}H-^{15}N HSQC spectra of the CD44 HABD in the absence of HA recorded at 25°C (top), 30°C (middle), and 37°C (bottom). Paired signals of the O conformation and the PD conformation are shown for T59 (right column) and G141 (left column), which are located at away from the HA-contact region. The relative intensities of the PD conformation signals with respect to the O conformation are shown in the spectra.

(B) N_{zz} exchange spectra of the ligand-free HABD, acquired without (black) or with a 500 ms mixing period (red). Cross peaks between the O and PD conformations were observed for residues such as G141 (upper spectrum), D23, I145, and V148 (lower spectrum), as indicated by dashed lines.

(C) Selected regions of the ^{1}H-^{15}N HSQC spectra of CD44 HABD in the HA-bound state, measured at 37°C. The relative intensities of the O conformation signals with respect to the PD conformation are shown in the spectra.

(D) Schematic drawings of the equilibrium of the CD44 HABD between the O conformation and the PD conformation. The size of the arrows drawn between the O state and the PD state are correlated with the changes in the conformational equilibrium in the presence and absence of HA.

the ligand-induced conformational change of the CD44 HABD is controversial and requires clarification.

In the present study, we demonstrated that CD44 HABD exchanges between the O and PD conformations in either the presence or absence of the HA ligand. The intrinsic two-state conformational transition of the HABD provides a clear explanation for the contradictory results between the X-ray and NMR structures, concerning the conformational rearrangement of the HABD upon HA binding. Furthermore, we prepared an engineered mutant that adopts only the PD conformation. This mutant exhibited higher affinity for HA, and when it was expressed on cell surfaces, the cells showed less efficient rolling behavior on the HA substrate under flow conditions. Based on these observations, we propose that the two-state equilibrium is essential for the CD44-mediated cell rolling.

RESULTS AND DISCUSSION

Conformational Equilibrium of CD44 HABD under the Physiological Conditions

In the previous study, we had completed the resonance assignment of all of the backbone signals of CD44 HABD in the ligand-free state that adopts the O conformation (Takeda et al., 2003). However, we noticed that a number of minor unassigned signals still remained on the HSQC spectrum (Figure 1A). The intensity ratios of those minor signals relative to the major signals exhibited a temperature-dependent increase, from 0.16 at 25°C to 0.64 at 37°C (Figure 1A). In addition, cross peaks were observed between the major and the minor signals in the N_{zz} exchange experiments at the mixing time of 500 ms (Figure 1B). Therefore, it was demonstrated that the HABD interconverts between two distinctive conformations with the exchange rate of hundreds of milliseconds. The chemical shifts of the minor signals in the ligand-free state mostly coincided with those of major signals in the HA-bound HABD state that adopts the PD conformation (Figures 1A and 1C). Likewise, the HSQC spectrum of the HA-bound HABD also provides minor signals at the position corresponding to the major signals of the HA-free state (Figure 1C). Based on these results, we conclude the CD44 HABD undergoes an equilibrium between the O and PD conformations, in either the presence or absence of HA, and the HA binding induces a shift of the equilibrium toward the PD conformation (Figure 1D).

Those results resolved the inconsistency regarding the conformation of the HABD in the HA-bound form, raised by previous X-ray and NMR studies (Banerji et al., 2007; Takeda et al., 2006). As demonstrated in this study, the HABD in the HA-bound form predominantly adopts the PD conformation, while the small fraction of the HA-bound HABD still adopts the O conformation. Therefore, under the physiological condition, both conformations, solved by the NMR and the X-ray crystallography, are present as a major and a minor population, respectively. Although less than 10% of the total HABD exists as the O conformation in the HA-bound state, it is likely that the sparsely populated O conformation was selectively crystallized because the PD conformation is unfavorable for crystallization, due to the flexibility of the C-terminal segment. In contrast, the major conformation in solution could be obtained in the structure determination by NMR of both the unbound (Teriete et al., 2004) and the HA-bound HABDs (Takeda et al., 2006), since the signal from the major conformation can be predominantly observed in NMR spectra.

The Y161A Mutant Constitutively Adopts the PD Conformation

In order to investigate the functional relevance of the two-state equilibrium of the CD44 HABD, we designed a mutant that would

influence the equilibrium. In comparison of the structures of the HABD in the unbound and HA-bound states, the most significant difference was found in the interactions between the C-terminal segment and the α1 helix of the Link module (Figures 2A and 2B). Specifically, the interactions of Tyr161 with Glu48 and Leu52 in the α1 helix seem to be critical for stabilizing the O conformation (Figure 2A). Therefore, we substituted Tyr with Ala at position of 161 and examined how the mutation modulates the conformational equilibrium of the HABD. The ^{1}H-^{15}N HSQC spectrum of the Y161A mutant exhibited a drastic change in the chemical shift pattern, as compared to the wild-type (WT) in the ligand-free state (Figure 2C), suggesting that the mutation induced global conformational changes of the HABD. As shown in some representative signals of Y161A, such as Thr59 and Gly141 (Figure 2C, insets), the cross peaks were observed only at the positions corresponding to those of WT in the HA-bound state. A comparison of the HSQC spectrum of Y161A with those of the unbound and HA-bound WTs revealed that the HSQC spectrum of Y161A in the unbound state more closely resembles that of WT in the HA-bound state (Figures 2D and 2E). Major differences in the signal patterns between Y161A in the free state and WT in the bound state were observed in limited regions, proximal to the site of the introduced mutation and the binding site of HA (Figure 2E). Therefore, Y161A adopts the PD conformation, which exhibits the disordered C-terminal segment, similar to the HA-bound form of WT. Furthermore, the results from the heteronuclear $\{^{1}H\}$-^{15}N NOE and trypsin limited digestion experiments demonstrated that the Y161A HABD in the unbound state had an enhanced flexibility at the C-terminal region (see Figure S1 available online), which is the hallmark of the PD conformation, as demonstrated in the WT HABD in the HA-bound state (Takeda et al., 2006). Taken together, we concluded that the Y161A mutant exclusively adopts the PD conformation.

Enhanced HA Affinity of the Y161A Mutant

We compared the HA-binding affinity of the WT and Y161A HABDs by surface plasmon resonance (SPR) experiments. The WT and Y161A HABDs were injected over a flowcell, where biotinylated HAs were immobilized via Streptavidin. From the curve fitting of the steady-state response over wide ranges of HABD concentrations (Schuck, 1997), the dissociation constant (K_D) of Y161A was estimated to be 3.3 ± 0.33 μM, which was 7-fold higher than that of WT, which was 24 ± 1.9 μM (Figures 3A and 3B). We could not obtain the kinetic parameters of the interaction between HA and both the WT and Y161A HABDs, since the SPR response curves could not be fitted by a 1:1 Langmuir binding model that assumes a single k_{on} and k_{off}. However, a comparison of the dissociation phases revealed that the dissociation of the Y161A HABD from the HA-immobilized surface was remarkably slower than that of WT (Figure 3C). This observation qualitatively indicates that the off rate of Y161A is slower than that of WT. Hence, the increased affinity of the Y161A mutant is, at least partially, due to its slower off rate.

Defect in Rolling Behavior for Cells Bearing Y161A Mutant

To investigate the significance of the two-state equilibrium on the cell adhesion and rolling, we prepared the transfectants expressing WT and Y161A CD44, using the lung carcinoma VMRC-LCD cell line, which lacks endogenous CD44 expression (Okamoto et al., 1999). Flow cytometric analysis showed that both transfectants express a comparable level of WT and Y161A CD44 (Figures 4A and 4B). The reactivity for the conformation-dependent antibodies indicated that the distinctive conformational rearrangement occurs in the HABD of the Y161A CD44 expressed on the cell surface (Figure S2). In the absence of flow, the adhesiveness of the Y161A cells was almost comparable with that of the WT cells, as shown by the results from the binding experiment to the soluble fluorescent-labeled HA (Figure 4C) and those from the cell binding assay to the HA-coated surface (Figure 4D). Therefore, the difference in the affinity of the individual receptor-ligand bond cannot be detected as the difference in the adhesiveness between the WT and Y161A cells under the static conditions because the multivalent interactions are stably formed between the cell surface CD44s and the HA substrate.

We examined the adhesiveness of the WT and Y161A cells under the fluid shear stresses using a glass capillary system in which undigested HA polymers were displayed on CD44-Ig-coated surfaces. The WT and Y161A cells were perfused at various shear stresses, ranging from 0.5 to 2.0 dyn/cm^2. After they became attached to the HA-coated surface, the WT cells smoothly rolled (Movie S1), as reported previously (DeGrendele et al., 1996). In contrast, the Y161A cells hardly moved on the surface (Movie S2). To quantify the differences in the adhesion behavior, the cells that moved more than or less than the cell diameter per 15 s interval were counted as "rolling" or "firm adhesion," respectively (Figure 5A). Overall, the cells bearing the WT CD44 mostly showed rolling behavior, while the cells bearing the Y161A CD44 mainly exhibited firm adhesion (Figure 5A). In addition, the total number of rolling and firm adhesion cells was greater for WT than for Y161A at all shear stresses (Figure 5A), suggesting that the WT CD44 can mediate new tether formation to HA more efficiently than Y161A. We also performed detachment assays (Figure 5B). Cells that accumulated at lower shear force were subjected to higher shear forces, which increased incrementally every 30 s, ranging from 0.5 to 16 dyn/cm^2, and the rolling velocity at each shear force was measured. The rolling velocity of the WT cells, which was 7 μm/s at the lower shear stress, increased up to 20 μm/s as the higher shear stress was applied (Figure 5B). In contrast, the Y161A cells showed substantially slower rolling velocities than the WT cells at all shear forces (Figure 5B).

To further characterize the differences in the rolling behavior between the WT and Y161A cells, we performed transient tether experiments using a parallel wall flow chamber system. The cells were perfused at 0.25 dyn/cm^2 under low HA concentration conditions, where no rolling can be observed, by lowering the amount of HA absorbed on the lower wall. In this experiment, the interaction between a single CD44 receptor on the cell surface and HA can be observed, as fewer multivalent interactions are formed, due to the lower density of the HA substrate. The number of cells showing transient tethering over the cells flowing on the HA-coated surface [tethering frequency (Dwir et al., 2000)] was greater for WT than Y161A (Figure 5C). This observation indicates that the WT cells possess better ability to form new receptor-ligand bonds and is consistent with the fact that the WT cells can

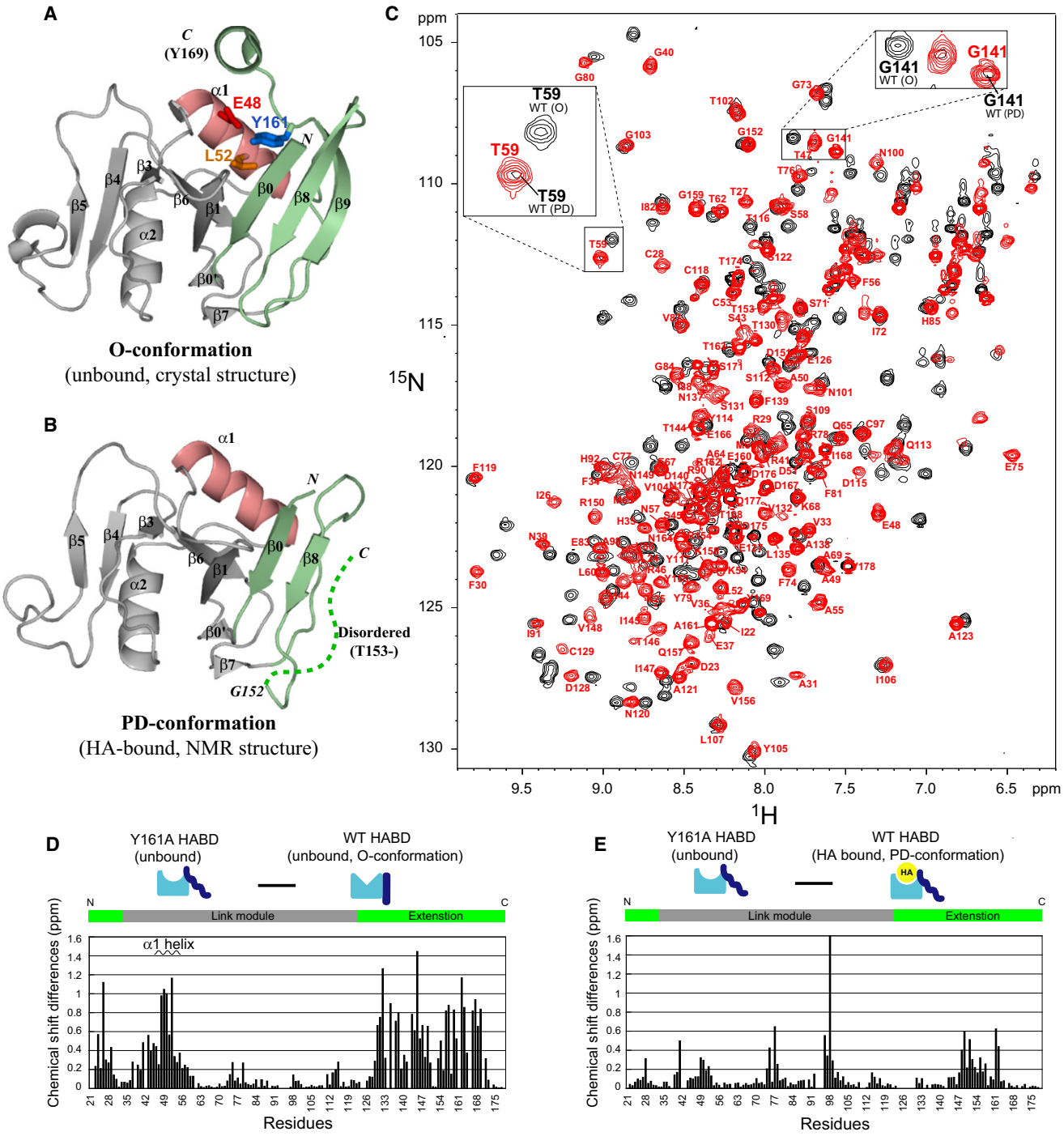

Figure 2. Change in the Conformational Equilibrium of the Y161A Mutant

(A) Crystal structure of the CD44 HABD in the HA-unbound state (PDB code: 1UUH). The Link module is colored gray and the extension segments are green. The α1 helix is colored red. The residues (E48, L52, and Y161) that are possibly involved in stabilizing the O conformation are indicated as sticks.

(B) NMR structure of CD44 HABD in complex with an HA hexamer (PDB code: 2I83). Color representation is the same as in (A). The C-terminal unfolded segment (T153 to Y169) is indicated by the dashed line. The C-terminal segment after G152 is not shown because of poor convergence in the NMR structure. These Figures were prepared with the PyMol software (DeLano Scientific).

(C) Overlaid ^{1}H-^{15}N HSQC spectra of WT (black) and Y161A HABD (red) in the ligand-free state. The signal assignments of Y161A are shown in red. Signals derived from T59 and G141 are shown in insets.

(D and E) Chemical shift differences between the ligand-free Y161A and the ligand-free WT (D) and the ligand-free Y161A and the HA-bound WT (E). The weighted averages of chemical shift differences (δΔ) were calculated using the equation $(\Delta\delta = [(\Delta\delta_{HN})^2 + (0.15\Delta\delta_N)^2]^{1/2})$ proposed by Mulder et al. (1999).

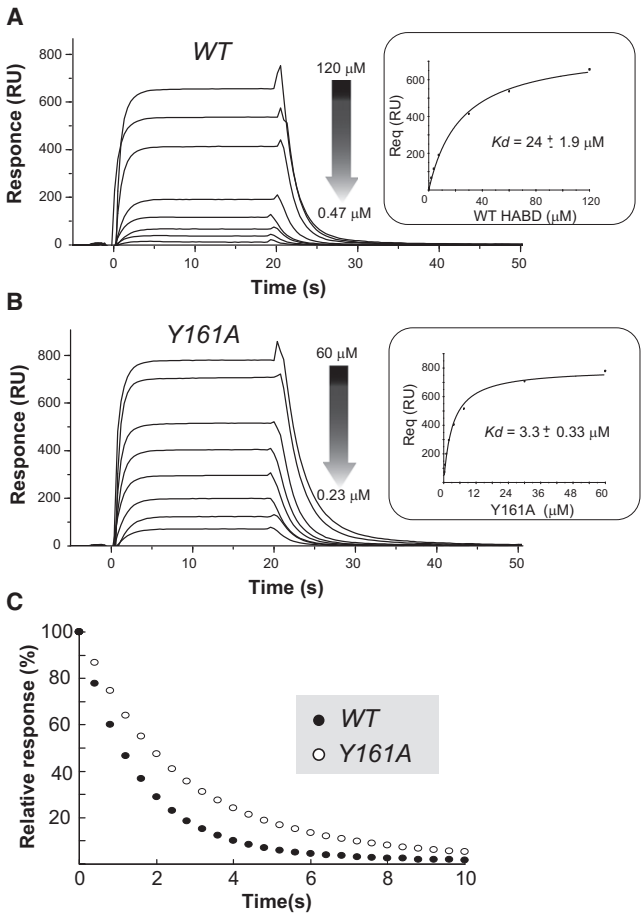

Figure 3. SPR Measurements of WT and Y161A HABD

(A and B) SPR sensorgrams of the WT (A; 0.47–120 μM) and Y161A HABDs (B; 0.23–60 μM) injected at 80 μl/min over the HA-immobilized and reference cells. The responses at equilibrium (R_{eq}) were plotted against the HABD concentrations (insets). K_D values were obtained by nonlinear curve fitting to a 1:1 binding isotherm.

(C) Comparison of the dissociation phase from HA between WT and Y161A. The time-dependent decays of the sensorgrams after the injection of 60 μM HABD are plotted for WT (closed circles) and Y161A HABD (open circles). Responses at the starting point of the dissociation phases are set to 100% for normalization.

support rolling more efficiently than the Y161A cells (Figure 5A). The number of cells showing tethering was plotted as a function of the duration of the tethers to determine the cellular off rate (Alon et al., 1995a). The cellular off rate was estimated to be 15.2 s^{-1} and 11.9 s^{-1} for WT and Y161A, respectively (Figure 5D), indicating that the increased adhesiveness of the Y161A cells is due to the prolonged lifetime of each receptor-ligand bond.

The Two-State Conformational Equilibrium of the HABD Is Crucial for CD44-Mediated Cell Rolling

In order for cells to roll along ligand-coated surfaces, the new bond formation at the edge of the rolling front and breakage at the rear edge need to occur continuously on an appropriate time scale (Thomas, 2008). Considering the fact that the majority of the CD44 HABD in the ligand-free state assumes the O conformation, which shows higher tethering frequency than the PD conformation, new ligand-receptor bonds would be efficiently formed at the rolling front (Figure 5E). As a result of the HA binding, the HABD undergoes the conformational change to the PD conformation, which is more resistant for the detachment force with the slower "cellular off rate." However, as we demonstrated in this study, the CD44 HABD in the HA-bound state still exists in an equilibrium between the O and PD conformations. Thus, the breakage of the receptor-ligand bond at the rear edge could be facilitated in a moment, when the conformation-liganded CD44 transitions to the O conformation (Figure 5E). We demonstrated that the two-state transition of the CD44 HABD occurs on the time scale of 100 ms by performing N_{zz} exchange experiments (Figure 1B). Furthermore, from line shape analyses, the exchange process between the O and PD conformations in the presence and the absence of HA was also estimated to be on the order of 100 ms (Figure S3). The dwell time of the cell surface CD44 on the HA substrate was estimated to be tens to hundreds of milliseconds (i.e., the inverse of the dissociation rate: $1/k_{off}$), determined from the transient tether experiments (Figure 5C). Therefore, the time scale of the conformational exchange of the HABD is comparable to the dwell time of the ligand-receptor bond formed on the cell surface. These findings support the hypothesis that, in rolling adhesion, the O conformation of the HABD could accelerate the dissociation of the receptor-ligand bond at the rear edge. In contrast, the Y161A mutant, in which the conformational equilibrium is eliminated, was defective in the rolling at all shear stresses tested in these experiments. Therefore, our study suggests that not only the increased affinity of the HABD but also the elimination of the two-state equilibrium would be responsible for the rolling defect of the Y161A cells, and thus emphasizes the importance of the conformational equilibrium for CD44-mediated rolling.

Allosteric Conformational Transition of CD44 and Other Rolling Receptors in the presence of Applied Forces

Our study on CD44 HABD is the first demonstration that an adhesion receptor exists in an equilibrium between the low-affinity and high-affinity conformations. In the previous studies, an allosteric conformational switch has been reported for adhesion molecules that mediate receptor-ligand interactions under flow conditions, such as selectins (Phan et al., 2006), the bacterial adhesin FimH (Thomas et al., 2002), and the I domain of the integrins (Shimaoka et al., 2003) (Figure S4), based on the crystal structures of the ligand-free and ligand-bound states. Although the existence of the equilibrium has not been experimentally examined, it is plausible that the two-state equilibrium could exist in those adhesion molecules. In addition, as demonstrated for CD44 in this study, the two-state equilibrium may play a crucial role for the rolling adhesion mediated by those receptors. In support of this, the mutations that destabilize the low affinity conformation were shown to abolish or impair the rolling mediated by selectins (Lou et al., 2006; Phan et al., 2006; Waldron and Springer, 2009), FimH (Thomas et al., 2002), and the αL-I domain (Salas et al., 2002).

Catch bonds are bonds that become stronger by the mechanical force pulling the ligand-receptor apart and their importance was recently demonstrated for the rolling adhesion mediated by L- and P-selectins and FimH (Marshall et al., 2003; Yakovenko et al., 2008). In the catch bond mechanism, the force exerted

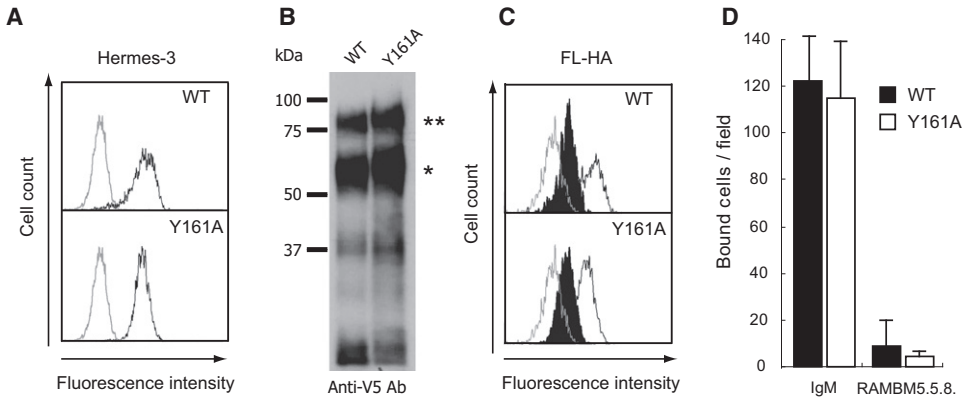

Figure 4. Characterization of the Cells Expressing WT and Y161A CD44

(A) Flow cytometry analysis of the VMRC-LCD cells expressing the WT or Y161A CD44, stained with the Hermes-3 anti-CD44 antibody (solid line). Mock cells stained under the same condition are shown as a gray solid line.

(B) Western blot analysis of the lysates of cells expressing the WT or Y161A CD44, detected with an alkaline phosphatase-conjugated anti-V5 mAb. Single and double asterisks indicate the two major bands of intact CD44 with different O-glycosylations.

(C) Flow cytometry of the parental VMRC-LCD cells (gray solid line) and the transfectants (black solid lines) incubated with 10 μg/ml fluorescein-labeled HA (FL-HA). The binding assay was performed in the presence of the anti-CD44 antibody RAMBM 5.5.8. (10 μg/ml; shaded profiles).

(D) Adhesion of VMRC-LCD transfectants to HA-immobilized cells on a flat bottom 24 well plate. The numbers of cells bound to the surface were counted by light microscopy. Average numbers of the WT cells (filled bars) and the Y161A cells (open bars) in the presence of either control or blocking IgM antibody were plotted with standard deviations from three experiments.

between the ligand-receptor is assumed to induce an allosteric conformational change, from the low- to high-affinity state (Thomas et al., 2008). Considering that the C-terminal segment of the CD44 HABD is connected to the plasma membrane, it might be possible that the force exerted between CD44 and HA could facilitate the conformational change from the O to the PD conformation. However, it should be noted that more than 90% of the CD44 HABD assumes the PD conformation upon HA binding in the absence of the applied force, as shown in our NMR study. Therefore, the effect of the force-induced equilibrium shift toward the PD conformation with the high affinity for HA could be less significant in the CD44-mediated cell adhesion.

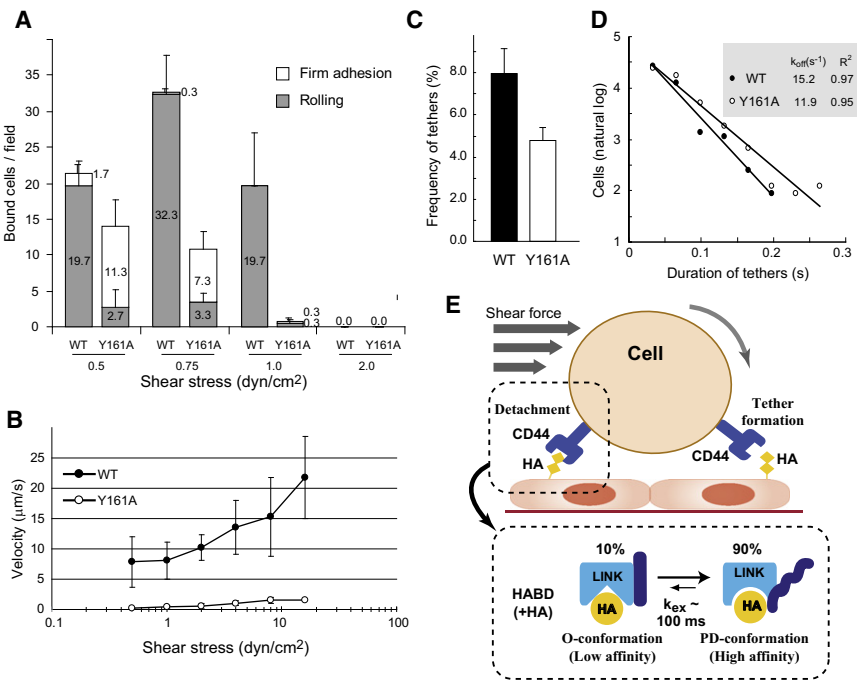

Figure 5. Rolling and Transient Tethering Assays of VMRC-LCD Transfectants Expressing CD44

(A) Adhesion of VMRC-LCD cells expressing the WT and Y161A CD44 under shear flow. Transfectants were allowed to accumulate on an HA-immobilized capillary for 10 min at the indicated shear stress. The numbers of rolling (dark bar) and firmly adherent (light bar) cells were measured at each shear stress.

(B) Mean velocity measured for transfectants bearing the WT (closed circles) or Y161A CD44 (open circles) in the detachment assay at increasing shear stress from 0.5 to 16 dyn/cm^2. Cells accumulated on the substrate at a shear stress of 0.5 dyn/cm^2, and then were subjected to shear forces increasing in 2-fold increments every 30 s.

(C) Frequency of transient tether formation for the WT (closed bar) and Y161A CD44 (open bar) expressing cells perfused in the flow chamber at a shear stress of 0.25 dyn/cm^2.

(D) Duration of transient tethers for the cells bearing the WT (closed circles) and Y161A CD44 (open circles). The natural logarithm of the number of cells was plotted as a function of the tether duration time to obtain the first-order dissociation kinetics (k_{off}) by a least square method. R^2 is the correlation coefficient. Data in (A)–(C) are shown as the average of three independent experiments (error bars, mean ± standard deviations).

(E) Schematics showing the significance of the two-state equilibrium of the CD44 HABD in the cell rolling. Detachment at the trailing edge would be facilitated by the conformational transition from the PD (high affinity) to the O (low affinity) conformation, which occurs at the time scale of 100 ms.

In conclusion, by altering the conformations of the regions away from the ligand-binding site, this study revealed that the CD44 HABD assumes two distinctive conformations that differ in ligand-binding affinity. In addition, CD44 HABD intrinsically exchanges between the low- and high-affinity conformations, in either the presence or absence of the ligand, on a time scale of hundreds of milliseconds. The results of the cell adhesion experiment under flow conditions proposed a structural basis for CD44-mediated cell rolling, in which the two-state equilibrium of the HABD between the high- and low-affinity states is crucial.

EXPERIMENTAL PROCEDURES

NMR Spectroscopy

^{15}N, $^{13}C/^{15}N$, and $^{2}H/^{15}N$-labeled WT and mutant CD44 HABDs (residues 21–178) were expressed and purified as described previously (Takeda et al., 2003). All NMR spectra [0.3–1.0 mM protein in 150 mM NaCl, 50 mM sodium phosphate (pH 6.7), 90% H_2O, and 10% D_2O] were recorded with Bruker Avance 500, 600, or 800 MHz spectrometers equipped with a cryogenic probe. ^{1}H-^{15}N HSQC spectra were collected at temperatures ranging from 15 to 37°C. The N_{zz} exchange spectra (Farrow et al., 1994) were acquired at 37°C with or without a mixing period of 500 ms using a $^{2}H/^{15}N$-labeled sample. Sequential assignments of the backbone resonances of the Y161A HABD were achieved with the following triple resonance experiments: HNCA, HNCACB, CBCA(CO)NH, HNCO, and HN(CA)CO. All spectra were processed by XWIN-NMR or Topsin (Bruker Biospin) and were analyzed by Sparky (Goddard and Kneller, 2008).

SPR Analyses

SPR experiments were performed using a BIACORE 2000 (GE Healthcare). HA was immobilized on the sensor chip SA, as described previously (Takeda et al., 2003). The binding assays were performed in the running buffer [150 mM NaCl and 50 mM sodium phosphate (pH 6.7)] at 25°C. Various concentrations of the WT (0.47−120 μM) and Y161A HABDs (0.23−60 μM) were injected into the flow cell at a flow rate of 80 μl/min. The K_D were obtained from the steady-state curve fitting analysis using the BIAevaluation 3.0 (GE Healthcare).

Generation of Stable Transfectants

The cDNA fragment encoding full-length CD44 was subcloned into pcDNA3.1/V5-His (Invitrogen). The Y161A mutant of CD44 was generated using the QuikChange method. VMRC-LCD cells were transfected with the vectors using Lipofectamine (Invitrogen), as reported previously (Okamoto et al., 1999), and were cultured in the medium containing 500 μg/ml G418 (GIBCO) to obtain stably transfected cells. The cells were cultured in RPMI 1640 medium (Sigma-Aldrich) supplemented with 10% fetal calf serum, 250 μg/ml G418, 1 mM sodium pyruvate, 2 mM L-glutamine, 100 U/ml penicillin, and 100 μg/ml streptomycin at 37°C in an atmosphere containing 5% CO_2.

Flow Cytometry Analysis

VMRC-LCD transfectants were stained with anti-CD44 mAbs (Hermes-1, Hermes-3, BU-75, 5F12, and IM7) for 20 min on ice, followed by FITC-labeled secondary antibody staining, and then were analyzed with either a EPICS XL (Beckman Coulter) or FACS Aria (Becton Dickinson) flow cytometer. Cell populations with high expression levels of WT and Y161A CD44, detected with Hermes-3, were used for cell adhesion assays under static and flow conditions. The binding of cell surface CD44 to FL-HA was analyzed as reported previously (Sugahara et al., 2003). Cells were preincubated with the anti-CD44 mAbs RAMBM 5.5.8 and BU-75 for control experiments.

Western Blotting

The lysates of the cultured cells were electrophoresed on a 10% SDS-polyacrylamide gel, and the proteins were transferred to a nitrocellulose membrane. The membrane was blocked with 10% skim milk and was then probed with a 1:2000 dilution of alkaline phosphatase-conjugated anti-V5 antibody (Invitrogen).

Cell Binding Assays

The 24 well plates (Falcon) were coated with 1 mg/ml HA at 4°C for overnight, and then were blocked with 2% BSA for 1 hr at room temperature. Suspensions of VMRC-LCD transfectants bearing WT or Y161A CD44 in 0.1% BSA/HBSS were incubated in each well for 10 min at room temperature. Control experiments were performed using the cells preincubated with RAMBM5.5.8. After several washes, the numbers of bound cells remaining in the wells were counted under the microscope.

Cell Adhesion Assays under Flow Conditions

Cell adhesion assays under flow conditions were performed as described by Nandi et al. (2000), with some modifications. The CD44-Ig fusion protein (46 μg/ml) was immobilized on the inside walls of glass capillaries (inner diameter, 0.69 mm; Drummond Scientific) at 4°C overnight. After three washes with PBS containing 0.01% (w/w) Tween-20, the capillaries were incubated with HA (1 mg/ml in PBS) for 3 hr at room temperature and then were blocked with PBS containing 2% BSA for 1 hr at room temperature. The capillaries were mounted on the stage of an inverted microscope (Diaphot 300; Nikon) with a 4× objective. The prepared transfectants, resuspended at 10^5 cells/ml in HBSS containing 0.1% BSA, were infused into the capillaries at shear forces ranging from 0.5 to 2.0 dyn/cm^2, as controlled by a PHD 2000 syringe pump (Harvard Apparatus). Ten minutes after the start of the infusion, cell images were recorded with a cell-viewing system (SRM-100; Nikon) and a video recorder (JVC BR-S600; Victor), and the number of rolling cells passing through a fixed plane (at the middle of the capillary tube from the entrance) perpendicular to the capillary axis was counted.

The results are expressed as the number of rolling cells per unit field. The cells that did not move more than one cell diameter in 15 s were defined as adhesion instead of rolling in this assay. For the detachment assays, the cells were allowed to accumulate for 15 min at 0.5 dyn/cm^2, and then the shear stress was increased stepwise every 30 s until it reached 32 dyn/cm^2. The rolling velocity at each shear stress was calculated from the average displacement of cells during a 10 s interval.

Transient Tethering

Biotinylated HA, prepared as described previously (Yu and Toole, 1995), was digested with hyaluronidase (Tawada et al., 2002) and subjected to the size exclusion chromatography to fractionate the chain length from approximately 8- to 34-mer. Polystyrene plates were coated with 10 μg/ml of NeutrAvidin (Pierce Biotechnology) in PBS (pH 9.0) at 4°C overnight, blocked at 4°C for 2 hr with 2% human serum albumin, and adsorbed with 5 μg/ml of the fragmented biotinylated HA in HBSS for 2 hr at 4°C. The plates were assembled as the lower wall in a parallel-wall flow chamber and were mounted on an inverted microscope. The transfectants were resuspended in HBSS containing 0.1% BSA and were perfused over the flow chamber at a density of 10^5 cells/ml and with a shear force of 0.25 dyn/cm^2. The frequency of tethering was determined as the number of tethering events divided by the number of cells transported across the field of view in the focal plane near the wall of the substrate (Fukuda et al., 2005). The number of tethering events at 0.033 s, as determined by the linear fit of the kinetics of the first 90% of transient tethers to dissociate, was used to calculate the tethering frequency (Chen and Springer, 2001).

SUPPLEMENTAL INFORMATION

Supplemental Information includes four figures and two movies and can be found with this article online at doi:10.1016/j.str.2010.02.010.

ACKNOWLEDGMENTS

We thank to T. Irimura and K. Denda for allowing us to use the flow cytometry facilities and S. Imai for providing scripts for image analysis. We are grateful for M. Osawa, M. Sakakura, and T. Ueda for useful discussion. This work was supported by grants from the Japan New Energy and Industrial Technology Development Organization and the Ministry of Economy, Trade, and Industry.

Received: December 19, 2009
Revised: February 13, 2010
Accepted: February 17, 2010
Published: May 11, 2010

REFERENCES

Alon, R., Hammer, D.A., and Springer, T.A. (1995a). Lifetime of the P-selectin-carbohydrate bond and its response to tensile force in hydrodynamic flow. Nature *374*, 539–542.

Alon, R., Kassner, P.D., Carr, M.W., Finger, E.B., Hemler, M.E., and Springer, T.A. (1995b). The integrin VLA-4 supports tethering and rolling in flow on VCAM-1. J. Cell Biol. *128*, 1243–1253.

Aruffo, A., Stamenkovic, I., Melnick, M., Underhill, C.B., and Seed, B. (1990). CD44 is the principal cell surface receptor for hyaluronate. Cell *61*, 1303–1313.

Banerji, S., Day, A.J., Kahmann, J.D., and Jackson, D.G. (1998). Characterization of a functional hyaluronan-binding domain from the human CD44 molecule expressed in Escherichia coli. Protein Expr. Purif. *14*, 371–381.

Banerji, S., Wright, A.J., Noble, M., Mahoney, D.J., Campbell, I.D., Day, A.J., and Jackson, D.G. (2007). Structures of the Cd44-hyaluronan complex provide insight into a fundamental carbohydrate-protein interaction. Nat. Struct. Mol. Biol. *14*, 234–239.

Chen, S., and Springer, T.A. (2001). Selectin receptor-ligand bonds: formation limited by shear rate and dissociation governed by the Bell model. Proc. Natl. Acad. Sci. USA *98*, 950–955.

Chen, S., Alon, R., Fuhlbrigge, R.C., and Springer, T.A. (1997). Rolling and transient tethering of leukocytes on antibodies reveal specializations of selectins. Proc. Natl. Acad. Sci. USA *94*, 3172–3177.

Clark, R.A., Alon, R., and Springer, T.A. (1996). CD44 and hyaluronan-dependent rolling interactions of lymphocytes on tonsillar stroma. J. Cell Biol. *134*, 1075–1087.

Day, A.J., and Prestwich, G.D. (2002). Hyaluronan-binding proteins: tying up the giant. J. Biol. Chem. *277*, 4585–4588.

DeGrendele, H.C., Estess, P., Picker, L.J., and Siegelman, M.H. (1996). CD44 and its ligand hyaluronate mediate rolling under physiologic flow: a novel lymphocyte-endothelial cell primary adhesion pathway. J. Exp. Med. *183*, 1119–1130.

Dwir, O., Kansas, G.S., and Alon, R. (2000). An activated L-selectin mutant with conserved equilibrium binding properties but enhanced ligand recognition under shear flow. J. Biol. Chem. *275*, 18682–18691.

Farrow, N.A., Muhandiram, R., Singer, A.U., Pascal, S.M., Kay, C.M., Gish, G., Shoelson, S.E., Pawson, T., Forman-Kay, J.D., and Kay, L.E. (1994). Backbone dynamics of a free and phosphopeptide-complexed Src homology 2 domain studied by 15N NMR relaxation. Biochemistry *33*, 5984–6003.

Fukuda, K., Doggett, T., Laurenzi, I.J., Liddington, R.C., and Diacovo, T.G. (2005). The snake venom protein botrocetin acts as a biological brace to promote dysfunctional platelet aggregation. Nat. Struct. Mol. Biol. *12*, 152–159.

Goddard, T.D., and Kneller, D.G. (2008). SPARKY 3. (http://www.cgl.ucsf.edu/home/sparky/).

Lou, J., Yago, T., Klopocki, A.G., Mehta, P., Chen, W., Zarnitsyna, V.I., Bovin, N.V., Zhu, C., and McEver, R.P. (2006). Flow-enhanced adhesion regulated by a selectin interdomain hinge. J. Cell Biol. *174*, 1107–1117.

Marshall, B.T., Long, M., Piper, J.W., Yago, T., McEver, R.P., and Zhu, C. (2003). Direct observation of catch bonds involving cell-adhesion molecules. Nature *423*, 190–193.

Mulder, F.A., Schipper, D., Bott, R., and Boelens, R. (1999). Altered flexibility in the substrate-binding site of related native and engineered high-alkaline Bacillus subtilisins. J. Mol. Biol. *292*, 111–123.

Nandi, A., Estess, P., and Siegelman, M.H. (2000). Hyaluronan anchoring and regulation on the surface of vascular endothelial cells is mediated through the functionally active form of CD44. J. Biol. Chem. *275*, 14939–14948.

Naor, D., Sionov, R.V., and Ish-Shalom, D. (1997). CD44: structure, function, and association with the malignant process. Adv. Cancer Res. *71*, 241–319.

Okamoto, I., Kawano, Y., Tsuiki, H., Sasaki, J., Nakao, M., Matsumoto, M., Suga, M., Ando, M., Nakajima, M., and Saya, H. (1999). CD44 cleavage induced by a membrane-associated metalloprotease plays a critical role in tumor cell migration. Oncogene *18*, 1435–1446.

Peach, R.J., Hollenbaugh, D., Stamenkovic, I., and Aruffo, A. (1993). Identification of hyaluronic acid binding sites in the extracellular domain of CD44. J. Cell Biol. *122*, 257–264.

Phan, U.T., Waldron, T.T., and Springer, T.A. (2006). Remodeling of the lectin-EGF-like domain interface in P- and L-selectin increases adhesiveness and shear resistance under hydrodynamic force. Nat. Immunol. *7*, 883–889.

Salas, A., Shimaoka, M., Chen, S., Carman, C.V., and Springer, T. (2002). Transition from rolling to firm adhesion is regulated by the conformation of the I domain of the integrin lymphocyte function-associated antigen-1. J. Biol. Chem. *277*, 50255–50262.

Schuck, P. (1997). Use of surface plasmon resonance to probe the equilibrium and dynamic aspects of interactions between biological macromolecules. Annu. Rev. Biophys. Biomol. Struct. *26*, 541–566.

Shimaoka, M., Xiao, T., Liu, J.H., Yang, Y., Dong, Y., Jun, C.D., McCormack, A., Zhang, R., Joachimiak, A., Takagi, J., et al. (2003). Structures of the alpha L I domain and its complex with ICAM-1 reveal a shape-shifting pathway for integrin regulation. Cell *112*, 99–111.

Sugahara, K.N., Murai, T., Nishinakamura, H., Kawashima, H., Saya, H., and Miyasaka, M. (2003). Hyaluronan oligosaccharides induce CD44 cleavage and promote cell migration in CD44-expressing tumor cells. J. Biol. Chem. *278*, 32259–32265.

Sugahara, K.N., Hirata, T., Hayasaka, H., Stern, R., Murai, T., and Miyasaka, M. (2006). Tumor cells enhance their own CD44 cleavage and motility by generating hyaluronan fragments. J. Biol. Chem. *281*, 5861–5868.

Takeda, M., Terasawa, H., Sakakura, M., Yamaguchi, Y., Kajiwara, M., Kawashima, H., Miyasaka, M., and Shimada, I. (2003). Hyaluronan recognition mode of CD44 revealed by cross-saturation and chemical shift perturbation experiments. J. Biol. Chem. *278*, 43550–43555.

Takeda, M., Ogino, S., Umemoto, R., Sakakura, M., Kajiwara, M., Sugahara, K.N., Hayasaka, H., Miyasaka, M., Terasawa, H., and Shimada, I. (2006). Ligand-induced structural changes of the CD44 hyaluronan-binding domain revealed by NMR. J. Biol. Chem. *281*, 40089–40095.

Tawada, A., Masa, T., Oonuki, Y., Watanabe, A., Matsuzaki, Y., and Asari, A. (2002). Large-scale preparation, purification, and characterization of hyaluronan oligosaccharides from 4-mers to 52-mers. Glycobiology *12*, 421–426.

Teriete, P., Banerji, S., Noble, M., Blundell, C.D., Wright, A.J., Pickford, A.R., Lowe, E., Mahoney, D.J., Tammi, M.I., Kahmann, J.D., et al. (2004). Structure of the regulatory hyaluronan binding domain in the inflammatory leukocyte homing receptor CD44. Mol. Cell *13*, 483–496.

Thomas, W. (2008). Catch bonds in adhesion. Annu. Rev. Biomed. Eng. *10*, 39–57.

Thomas, W.E., Trintchina, E., Forero, M., Vogel, V., and Sokurenko, E.V. (2002). Bacterial adhesion to target cells enhanced by shear force. Cell *109*, 913–923.

Thomas, W.E., Vogel, V., and Sokurenko, E. (2008). Biophysics of catch bonds. Annu. Rev. Biophys. *37*, 399–416.

Tsukita, S., Oishi, K., Sato, N., Sagara, J., and Kawai, A. (1994). ERM family members as molecular linkers between the cell surface glycoprotein CD44 and actin-based cytoskeletons. J. Cell Biol. *126*, 391–401.

Waldron, T.T., and Springer, T.A. (2009). Transmission of allostery through the lectin domain in selectin-mediated cell adhesion. Proc. Natl. Acad. Sci. USA *106*, 85–90.

Yakovenko, O., Sharma, S., Forero, M., Tchesnokova, V., Aprikian, P., Kidd, B., Mach, A., Vogel, V., Sokurenko, E., and Thomas, W.E. (2008). FimH forms catch bonds that are enhanced by mechanical force due to allosteric regulation. J. Biol. Chem. *283*, 11596–11605.

Yu, Q., and Toole, B.P. (1995). Biotinylated hyaluronan as a probe for detection of binding proteins in cells and tissues. Biotechniques *19*, 122–124, 126–129.

